



Deep Network Pruning: A Comparative Study on CNNs in Face Recognition

Fernando **Alonso-Fernandez**^{a,b,**}, Kevin **Hernandez-Diaz**^a, Jose Maria **Buades Rubio**^b, Prayag **Tiwari**^a, Josef **Bigun**^a

^a*School of Information Science, Computer and Electrical Engineering, Halmstad University, Box 823, Halmstad SE 301-18, Sweden*

^b*Computer Graphics and Vision and AI Group, University of Balearic Islands, Spain*

Article history:

Keywords: Face Recognition, Mobile Biometrics, Network Pruning, Taylor Expansion, Deep Learning, Convolutional Neural Networks

ABSTRACT

The widespread use of mobile devices for all kind of transactions makes necessary reliable and real-time identity authentication, leading to the adoption of face recognition (FR) via the cameras embedded in such devices. Progress of deep Convolutional Neural Networks (CNNs) has provided substantial advances in FR. Nonetheless, the size of state-of-the-art architectures is unsuitable for mobile deployment, since they often encompass hundreds of megabytes and millions of parameters. We address this by studying methods for deep network compression applied to FR. In particular, we apply network pruning based on Taylor scores, where less important filters are removed iteratively. The method is tested on three networks based on the small SqueezeNet (1.24M parameters) and the popular MobileNetv2 (3.5M) and ResNet50 (23.5M) architectures. These have been selected to showcase the method on CNNs with different complexities and sizes. We observe that a substantial percentage of filters can be removed with minimal performance loss. Also, filters with the highest amount of output channels tend to be removed first, suggesting that high-dimensional spaces within popular CNNs are over-dimensioned.

© 2024 Elsevier Ltd. All rights reserved.

1. Introduction

Mobile biometrics can offer secure, user-friendly authentication for many services such as e-commerce, banking, messaging, remote work, social media, education, healthcare, government services, etc. Here, we address face recognition (FR), where Convolutional Neural Networks (CNN), as in many other vision tasks, have become the popular tool [Sundararajan and Woodard, 2018]. Given enough data, CNNs produce classifiers with impressive performance in unconstrained scenarios with high variability. However, the limited computational resources of mobile devices makes that popular CNNs are often unsuitable due to their complexity and large model sizes. This creates the challenge of developing lighter and more efficient models that maintain accuracy without the heavy resource requirements.

There is, therefore, interest in developing light biometric CNNs, driven by the need for authentication on devices with

limited processing. Here, we apply network compression [Caldeira et al., 2024] to existing popular CNN architectures to create more compact models without sacrificing accuracy. We use a pruning method based on importance scores of network filters [Molchanov et al., 2019], which quantifies the impact on the network error if filters are removed. Such scores are obtained via first-order Taylor approximation, which only requires the gradient elements from backpropagation.

In an earlier work [Alonso-Fernandez et al., 2023], we used this method to reduce an already small SqueezeNet network of 1.24M parameters [Iandola et al., 2016; Alonso-Fernandez et al., 2020]. Such work was among the first ones to evaluate network pruning for FR [Caldeira et al., 2024]. This paper extends the study to MobileNetv2 [Sandler et al., 2018] (3.5M parameters) and ResNet50 [He et al., 2016] (23.5M). Such architectures are selected to consider a different amount of model sizes. The purpose and contributions of this work are, therefore, multi-fold. We first summarize literature in network compression, in particular pruning for FR. Then, we study the impact of the employed pruning method on the FR performance of three different-sized CNN architectures. In our experiments,

^{**}Corresponding author: Fernando Alonso-Fernandez (feralo@hh.se). Under consideration at *Pattern Recognition Letters*.

we prune to up to 99% of the filters, maintaining performance until a certain percentage. SqueezeNet and MobileNetv2 allow up to 20-30% pruning, situating them at $\sim 1\text{M}$ parameters. The larger ResNet50 allows up to 99% pruning in some cases which, interestingly, also corresponds to $\sim 1\text{M}$ parameters. We also analyze the effect of pruning in network layers, observing that those with most channels are pruned first.

2. Related Works

Several light CNNs have been presented across the years [Iandola et al., 2016; Sandler et al., 2018; Zhang et al., 2018; Tan and Le, 2019; Zhang et al., 2020], mainly for generic visual tasks in the context of ImageNet [Russakovsky et al., 2015], using techniques that allow faster processing and fewer parameters such as point-wise convolution, depth-wise separable convolution, variable group convolution, mixed convolution, channel shuffle, and bottleneck layers. Some have been used for FR, either in their original form, or reducing channels or layers for compactness [Chen et al., 2018; Duong et al., 2019; Martinez-Díaz et al., 2019; Yan et al., 2019; Alonso-Fernandez et al., 2020; Boutros et al., 2021]. In doing the latter, however, the number of channels or layers is reduced heuristically just to obtain a more compact network.

Instead of manual adaptation, the work [Boutros et al., 2022] suggested Neural Architecture Search (NAS) to design light FR models named PocketNets. Another increasingly used strategy is network compression. Most biometrics-related compression works have focused on FR, with some others applied to ocular recognition [Almadan and Rattani, 2023], face detection [Jiang et al., 2022], and, to a minor extent, iris, expression, emotion, morphing attacks, or sclera segmentation [Caldeira et al., 2024]. Compression techniques include quantization, knowledge distillation (KD) and pruning. Model quantization converts full-precision (FP) weights and activations (typically in 32 bits) to a lower precision (LP) of 8 bits to up to 1 bit, maintaining the same architecture. LP is less computationally expensive, and several hardware and libraries are optimized for fast 8 bit processing. KD uses a teacher network, usually a complex model that performs well in the proposed task, to guide a lighter student model. The student is trained to produce the output of the teacher via loss functions that minimize the gap between their responses. However, as with quantization, the architecture of KD networks is fixed. In network pruning, on the other hand, redundant parts or connections are eliminated, resulting in a more sparse network. To do so, network weights are usually ordered according to some criteria, and those with the lowest importance are removed until the desired level of sparsity.

Most network compression literature for FR and biometrics in general uses KD [Caldeira et al., 2024]. Apart from our mentioned work [Alonso-Fernandez et al., 2023], few have applied pruning [Polyak and Wolf, 2015; Liu et al., 2022]. The paper [Polyak and Wolf, 2015] proposed two methods to remove low contributing channels: inbound pruning (IP) and reduce and reuse pruning (RRP). IP prunes inbound channels of a layer, whereas RRP prunes outbound channels. The importance of a channel is determined by the variance of its activa-

tions. Connections with low variance are deemed as less important, so they can be removed. They also considered hybrid pruning (HP) by first applying RRP followed by IP. The methods were tested on CASIA and LFW datasets, improving runtime up to 2.65 with less than a 2% accuracy drop. The work [Liu et al., 2022] proposed a method to remove channels using a loss function with two terms: a reconstruction error between the feature maps of the baseline network and the pruned one, and a discrimination-aware term that uses the output of intermediate layers as features to do the actual softmax classification. FR experiments used LResNet34E-IR and Mobile-FaceNet as backbones (trained on MS-Celeb-1M) and four well-known benchmark datasets (LFW, CFP-FP, AgeDB-30, and MegaFace), showing negligible performance drops after pruning 25-50% of the channels.

3. Materials and Methods

3.1. Network Pruning

We apply the method for general network pruning of [Molchanov et al., 2019]. It iteratively estimates the importance scores of individual elements based on their effect on the network loss. Then, elements with the lowest scores are pruned, resulting in a more compact network. Given a network with parameters $\mathbf{W} = \{w_0, w_1, \dots, w_M\}$ and a training set \mathcal{D} of input (x_i) and output (y_i) pairs $\mathcal{D} = \{(x_0, y_0), (x_1, y_1), \dots, (x_K, y_K)\}$, the aim of network training is to minimize the classification error E by solving

$$\min_{\mathbf{W}} E(\mathcal{D}, \mathbf{W}) = \min_{\mathbf{W}} E(y|x, \mathbf{W}) \quad (1)$$

The importance of a parameter w_m can be defined by its impact on the error if it is removed. Under an *i.i.d.* assumption, the induced error can be quantified as:

$$\mathcal{I}_m = \left(E(\mathcal{D}, \mathbf{W}) - E(\mathcal{D}, \mathbf{W}|w_m = 0) \right)^2 \quad (2)$$

Computing \mathcal{I}_m for each parameter would demand to evaluate M versions of the network, making the process expensive. This is avoided by approximating \mathcal{I}_m in the vicinity of \mathbf{W} by its first-order Taylor expansion:

$$\mathcal{I}_m^1(\mathbf{W}) = (g_m w_m)^2 \quad (3)$$

where $g_m = \frac{\partial E}{\partial w_m}$ are the elements of the gradient g . A second-order expansion is also possible via the Hessian of E [Molchanov et al., 2019], but we employ the first-order approximation for faster computation. The gradient g is available from backpropagation, so \mathcal{I}_m^1 can be easily computed. The joint importance of a set of parameters \mathbf{W}_S (e.g. a filter) can then be obtained as:

$$\mathcal{I}_S^1(\mathbf{W}) \triangleq \sum_{s \in S} (g_s w_s)^2 \quad (4)$$

The algorithm starts with a trained network, which is pruned iteratively over the same training set. Given a mini-batch, the gradients are computed, the network weights are updated by

Table 1: Networks evaluated in this paper.

Model	Conv Layers	Total Filters	Model Size	Para-meters	Vector Size
SqueezeNet	18	3168	4.6MB	1.24M	1000
MobileNetv2	53	7950	13MB	3.5M	1280
ResNet50	50	21274	83.9MB	23.5M	2048

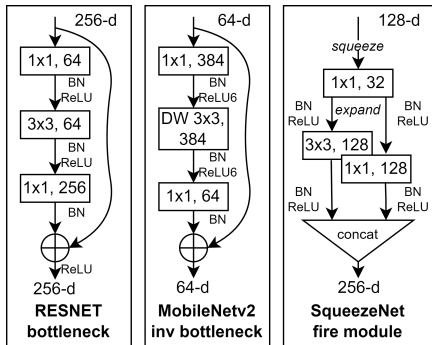


Fig. 1: Internal architecture of the building blocks of the CNN architectures employed. Inspired by [He et al., 2016].

gradient descent, and the importance of each filter is obtained via Eq. 4. At the end of each epoch, the scores of each filter are averaged over the mini-batches, and those with the smallest importance are removed. The resulting network can be then fine-tuned again to regain potential accuracy losses.

3.2. Recognition Architectures

We use three CNNs, chosen to account for a different number of parameters or depth (Table 1). They comprise two light architectures (SqueezeNet, MobileNetv2), and a large ResNet50. *ResNet* networks [He et al., 2016] introduced residual connections, allowing the input from a lower layer to reach a higher layer, bypassing intermediate ones. Followed later by many (including MobileNet), this allows deeper networks and eases training by improving gradient propagation. The authors also introduced bottleneck blocks (Figure 1, left) where high input dimensionality is first reduced with 1×1 point-wise filters, then 3×3 filters are applied over the lower dimensional space, and finally 1×1 filters regain the input dimensionality. The larger 3×3 filters are applied in the reduced dimensionality space, resulting in fewer parameters. We use the ResNet50 variant with 50 convolutional layers, 23.5M parameters, and 83.9 Mb. *MobileNetv2* [Sandler et al., 2018] uses depth-wise separable convolutions and inverted residuals to achieve a light architecture (3.5M parameters, 13Mb and 53 convolutional layers). In inverted residuals (Figure 1, center), also called inverted bottleneck blocks with expansion, channel dimensionality is first expanded (instead of reduced) with 1×1 filters. Then, 3×3 filters are applied, but to cope with the increased dimensionality, they are implemented via depth-wise separable convolution for parameter and processing savings. Finally, channel dimensionality is reduced again with 1×1 filters. *SqueezeNet* [Iandola et al., 2016] is among the smallest architectures proposed within ImageNet (18 convolutional layers, 1.24M parameters, and 4.6 MB), and one of the early attempts to reduce the net-

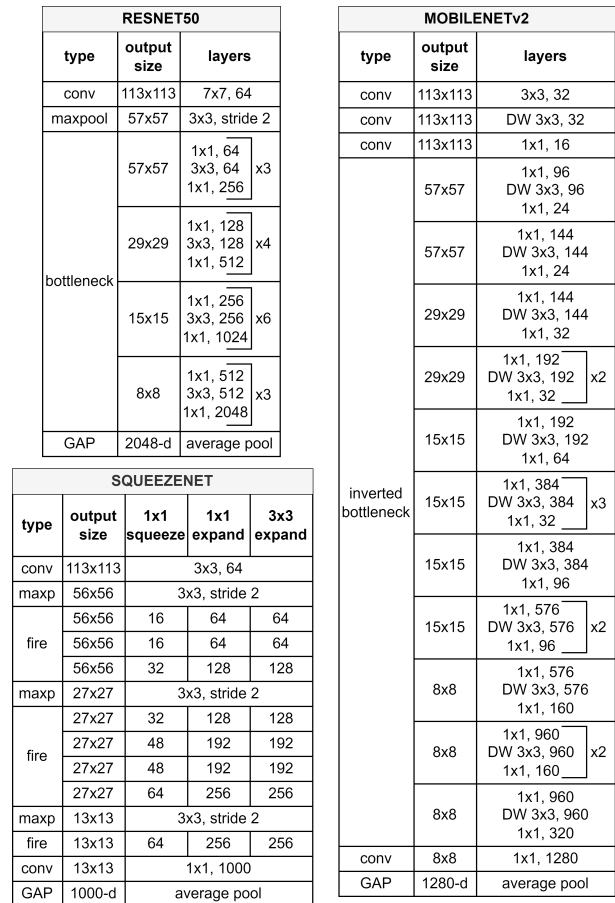


Fig. 2: Architecture of the networks used.

work parameters and size. It uses *squeeze* and *expand* steps, similar to bottlenecks, but with a stack of two layers only called *fire* module (Figure 1, right). The channel dimensionality is first *squeezed* with 1×1 point-wise filters, and then *expanded* with a larger amount of 3×3 and 1×1 filters. SqueezeNet uses late downsampling to keep larger activation maps as much as possible, and it is a sequential CNN without residuals.

Figure 2 shows the architecture of the three networks, from our training environment (Matlab r2023b), with slight changes. The networks use a 113×113 input, achieved by changing the stride of the first convolutional layer from 2 to 1, which keeps the rest of the network unchanged. This allows reusing ImageNet pre-trained networks as starting models for faster convergence [Kornblith et al., 2019]. SqueezeNet uses ReLU activation, and we have added batch normalization (missing in the original implementation), since it helps to improve performance [Alonso-Fernandez et al., 2023]. Bottleneck blocks in ResNet50 include batch normalization and ReLU. MobileNetv2 uses ReLU6 as non-linearity (clipped ReLU), but only after the first two convolutions of inverted bottlenecks.

3.3. Databases

VGGFace2 [Cao et al., 2018] is used for training and evaluation, comprising 3.31M images of 9131 celebrities (362.6 images per person on average). The images are sourced from the internet, with significant variations in pose, age, ethnicity,

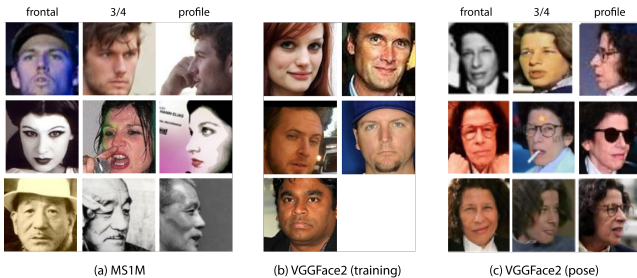


Fig. 3: Example images of the databases used. (a) MS1M from three users (by row) and three viewpoints (column). (b) VGGFace2 training images with a random crop. (c) VGGFace2 pose templates from three viewpoints (by column).

Table 2: Number of biometric verification scores. Same pose experiments include three types (which explains the $3 \times$ term): frontal vs. frontal, 3/4 and profile vs. profile. Similarly, cross-pose experiments include: frontal vs. 3/4, frontal vs. profile, and 3/4 vs. profile.

Template	Type	Same pose	Cross pose	Total
1-1	Genuine	$3 \times 368 \times (9+8+\dots+1)$	$3 \times 368 \times 10 \times 10$	160,080
	Impostor	$3 \times 368 \times 100$	$3 \times 368 \times 100$	220,800
5-5	Genuine	$3 \times 368 \times 1$	$3 \times 368 \times 2 \times 2$	5,520
	Impostor	$3 \times 368 \times 100$	$3 \times 368 \times 100$	220,800

lighting, and background. The data is divided into 8631 training classes (3.14M images) and 500 testing classes. A subset of 368 subjects from the test set is defined, VGGFace2-Pose, with 10 images per pose (frontal, three-quarter, profile) and 11040 images. To improve performance, we pre-train the networks with the RetinaFace cleaned subset of MS-Celeb-1M [Guo et al., 2016] (referred to as MS1M), which includes 5.1M images of 93.4K identities. The images are cropped to 113×113 using the five RetinaFace landmarks [Deng et al., 2019b]. While MS1M has more images, its intra-identity variation is limited due to an average of 81 images per person. We address this by pre-training on MS1M, and then fine-tuning on the more diverse VGGFace2. This demonstrated to yield superior performance compared to training on VGGFace2 only [Cao et al., 2018; Alonso-Fernandez et al., 2020]. Some examples of the databases are shown in Figure 3.

3.4. Training and Verification Protocols

The networks are trained for biometric identification with soft-max and the ImageNet weights as initialization. Training and evaluation follow the VGGFace2 protocol [Cao et al., 2018]. During training, the shortest side of VGGFace2 bounding boxes is resized to 129 pixels and then a random 113×113 crop is taken. MS1M images are directly at 113×113 . Additionally, we apply a horizontal random flip. Our optimizer is SGDM with a mini-batch of 128. The learning rate starts at 0.01 and is reduced to 0.005, 0.001, and 0.0001 when the validation loss plateaus. We reserve 2% of images per user in the training set for validation. MS1M users with fewer than 70 images are excluded to avoid fully connected layers dedicated to under-represented classes, resulting in 35016 users and 3.16M images. Our training environment is Matlab r2023b.

We conduct verification experiments with VGGFace2-Pose resizing the shortest image side to 129 pixels, then taking a centre 113×113 crop. VGGFace2-Pose allows same-pose and

cross-pose comparisons. Genuine (mated) scores are obtained by comparing each template of a user to his/her remaining ones, avoiding symmetric comparisons. For impostor (non-mated) scores, the first template of a user is used as enrolment and compared with the second template of the next 100 users. Identity templates are created by combining five faces of the same pose [Cao et al., 2018], leading to two templates per user and pose. To test the robustness of the network and the pruning under more challenging conditions, we also use single-image templates. Template vectors are created by averaging face descriptors from the Global Average Pooling layer. To combat pose variation, we average the descriptor of an image with its horizontally flipped counterpart [Duong et al., 2019]. The cosine similarity is used for template comparison. Table 2 shows the total number of scores.

4. Results and Discussion

We apply pruning to the networks using a random 25% of the VGGFace2 training set to compute the filter importance scores. We then remove 1% of the lowest-scoring filters after each epoch. The optimizer is SGDM with mini-batch 128 and learning rate 0.01. Figure 4 (blue curves) shows the EER of the pruned networks on VGGFace2-Pose. The baseline EER at $x=0$ (no pruning) is 6.07% (SqueezeNet), 3.75% (MobileNetv2) and 3.84% (ResNet50) in one-to-one comparisons (single-image template), and 0.52%, 0.14% and 0.13% for five-to-five comparisons. The deeper MobileNetv2 and ResNet50 outperform the lighter SqueezeNet, with MobileNetv2 matching or exceeding ResNet50 with fewer parameters and size, demonstrating the effectiveness of the MobileNetv2 design to provide good accuracy with a reduced network.

After just removing 1% of the filters (first iteration), a sharp increase in error rates occurs. We attribute this to overfitting since the networks have been trained previously over the same set with early stopping. After this jump, performance stabilizes or improves until a certain percentage of the filters are pruned, but the behaviour differs substantially per network. SqueezeNet maintains performance until 15-20% pruning (in five-to-five comparisons, until 40%, albeit with some oscillations). MobileNetv2, on the other hand, is very sensitive to filter removal, and performance drops substantially after 10% pruning. ResNet50 remains stable even after 60-70% pruning, showing its robustness to filter removal. However, even with 70% filters removed, ResNet50 has more parameters than the other networks, as it will be analyzed later.

To regain accuracy losses, pruned networks are retrained again on VGGFace2. The results are given in Figure 4 as well. We use a starting learning rate of 0.01 (red curve) and 0.001 (orange). We hypothesise that, since the network has been already trained on the same database, starting with a high rate may be counterproductive. However, this is not the case, since the best results are with a starting rate of 0.01. All architectures maintain accuracy up to a certain pruning percentage. In addition, using five images per template allows higher pruning sparsities. Combining several images may produce that the most relevant features of each identity are kept, while random infor-

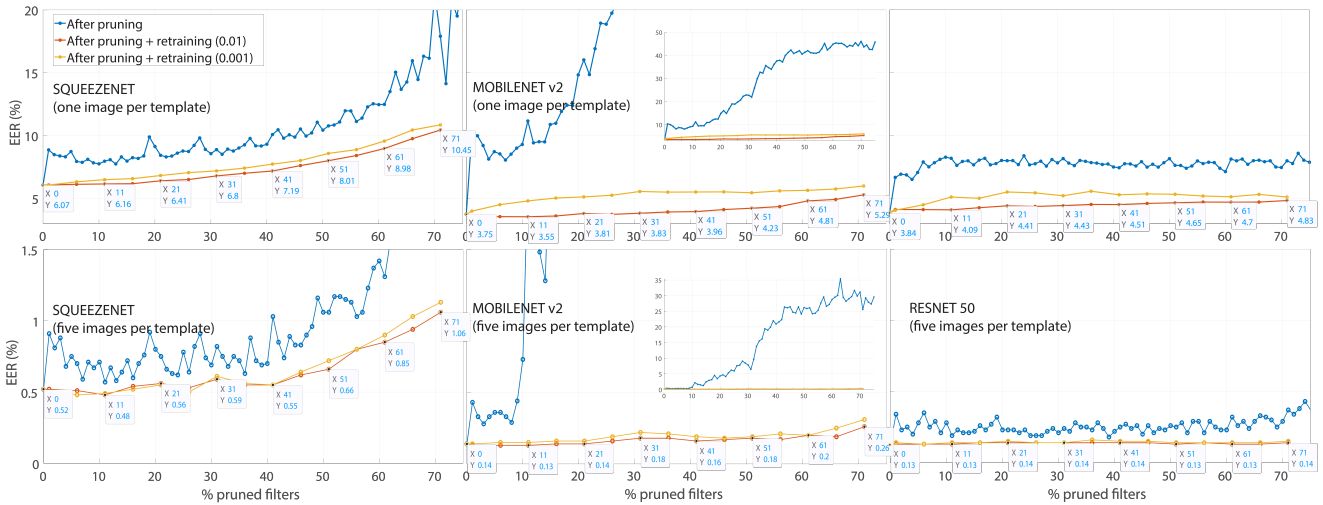


Fig. 4: Face verification results on the VGG2-Pose database (EER %) over the network pruning process. Data tips show selected values of the red curve (after pruning + retraining at 0.01).

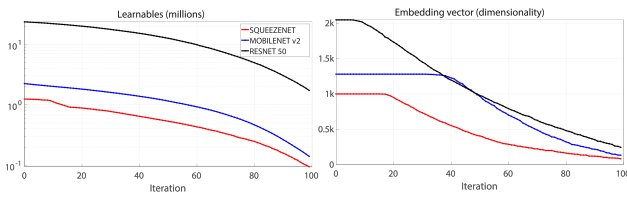


Fig. 5: Effect of pruning in the network (learnables and embedding size).

information is averaged out [Caldeira et al., 2024]. However, similarly as above, the behaviour per network differs. SqueezeNet maintains performance until 15-20% (one-to-one) or 20-30% pruning (five-to-five). ResNet remains stable even with high pruning, and the performance gap w.r.t. the unpruned network is eliminated. On the other hand, the sensitiveness of MobileNet2 to pruning is substantially reduced after retraining, maintaining a stable performance until 20-30% pruning in both one-to-one and five-to-five comparisons. At 40% or 50% pruning, it remains competitive, and on par or even better than the bigger ResNet50. Indeed, the EERs of MobileNet2 are consistently smaller than ResNet50 (especially in one-to-one comparisons), suggesting that MobileNet2 is a very robust architecture with capabilities comparable to much larger networks.

We analyze pruning effect on the networks themselves by plotting learnables and embedding dimensionality (Figure 5). In all networks, learnables decrease slowly until 20-30% of the filters are removed, then the decrease is sharper, so the filters that are removed first do not affect a high amount of channels. There is a small exception with SqueezeNet, which has a pronounced drop between 10-15%, but the decrease stabilizes afterwards. Embedding size remains constant until certain pruning levels which, again, is different per network. ResNet50 starts reducing its output dimensionality with less than 10% pruning, SqueezeNet at $\sim 20\%$, and MobileNet2 at $\sim 40\%$. A reduction in the embedding indicates that pruning affects the last layer. Such layer is supposed to be the more specific for the task, so it could be expected that it is not affected in the early pruning stages [Caldeira et al., 2024]. However, this does

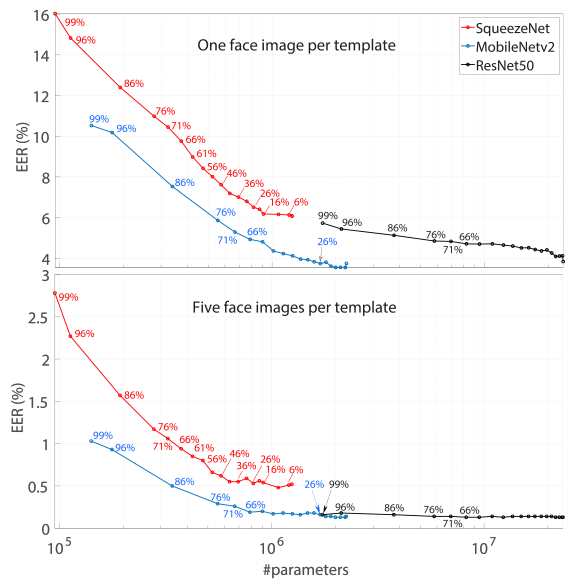


Fig. 6: Verification accuracy on VGG2-Pose (ERR %) vs. amount of learnables. The labels in the curves indicate the corresponding percentage of pruned filters.

not hold with ResNet50. Nevertheless, ResNet50 is substantially bigger (Table 1), its embedding duplicates others (2048 vs. 1280 or 1000), but its performance is not substantially better (Figure 4). Research has shown that feature spaces of 512 or 1024 contain sufficient degrees of freedom to encode a face, allowing further reduction with minor accuracy drops [O’Toole et al., 2018]. Thus, it is reasonable that the large ResNet50 embedding is affected from the beginning.

The latter observations suggest that ResNet50 is overdimensionated on several aspects. At 71% pruning, it has ten times more parameters than MobileNet2 (6.97M vs. 0.67M), but not significantly better accuracy: 4.83% vs. 5.29% in one-to-one comparisons (8.7% decrease), or 0.15% vs. 0.31% in five-to-five comparisons (51.6% decrease). Indeed, at 99% pruning, ResNet50 learnables are comparable to MobileNet2 without any pruning. To better analyze this effect, we plot in

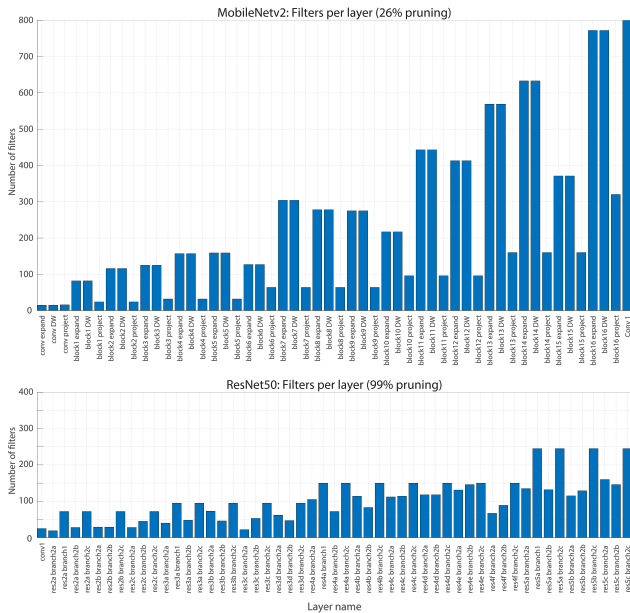


Fig. 7: MobileNetV2 and ResNet50 structure after 26% and 99% pruning respectively. The layer names correspond to the networks’ release of Matlab r2023b. The last layer of MobileNetV2 has 1280 filters (capped for visualization purposes).

Figure 6 the accuracy against the number of learnables. In one-to-one comparisons, when ResNet50 and MobileNetV2 have similar parameters ($\sim 1.07M$), MobileNetV2 has a 2% smaller EER. This occurs when MobileNetV2 is pruned at 26% and ResNet50 at 99%. Despite similar depth (conv layers) and parameters, MobileNetV2 seems *fundamentally* better. Figure 7 shows the filters per layer of MobileNetV2 at 26% pruning and ResNet50 at 99%. ResNet50 layers mostly have less than 150 filters, even in the last stage of bottleneck layers originally designed to increase dimensionality by $4\times$ (those containing ‘branch2c’ in the name). Also, the last part of the network has 250 filters, which contrasts to the 2048 of the unpruned network. On the other hand, MobileNetV2 maintains a more prominent difference inside bottlenecks. Also, filter count increases substantially towards the end of the network, when the layers are supposed to be more specific for the task, which may explain its superior performance w.r.t. ResNet50.

Interestingly, in the 1-1.1M parameters range, ResNet50 (99% pruned) and SqueezeNet ($<10\%$ pruned) perform similarly, despite the simpler structure of SqueezeNet. However, the smaller embedding size of ResNet50 (245 elements, Figure 5) vs. SqueezeNet (1000) suggests that the most intricate structure of ResNet can provide similar performance with a smaller embedding. On the other hand, differences between ResNet50 and MobileNetV2 disappear with five images per template (bottom plot of Figure 6), compensating for the observed limitations of ResNet50. It can be also seen that the gap of SqueezeNet remains in five-to-five comparisons, showing the limitations of such a simpler architecture.

We further analyze the effect of pruning on the networks by plotting (Figure 8) the filters per layer for different pruning degrees (up to 20%). Filters removed first (marked with black circles) belong to layers with the most channels, which are ded-

icated to dimensionality increase. Similarly to the embedding size, these high-dimensional spaces seem over-dimensioned for the task. This is obviously more prominent in the network with the biggest dimensional spaces (ResNet50). At 20% pruning, ResNet50 layers of original dimensionality 2048, 1024, and 512 are reduced to less than 1000, 540, and 255 channels respectively (less than half). This aligns with previous findings (Figure 7) showing reduced dimensionality differences inside ResNet50 bottlenecks throughout pruning. Thus, it makes sense that high-dimensional channels are affected the most.

5. Conclusions

Popular face recognition technologies use large Convolutional Neural Networks (CNNs) [Sundararajan and Woodard, 2018] with hundreds of megabytes and/or millions of parameters, which can be impractical for low-capacity hardware. We are thus interested in methods to achieve lighter CNN architectures without sacrificing performance. Here, we explore the application of a network pruning method based on Taylor scores which only require the backpropagation gradient to measure the impact of filters on the classification error. This allows iterative removal of least contributing filters. The method is evaluated on three architectures with varying parameters and depth. Each network allows a different degree of pruning without substantial performance loss, based on its initial size. For example, the heaviest architecture allows up to 99% pruning, while the second heaviest allows below 30%. However, at these points, both have similar learnables ($\sim 1M$) and performance. Thus, larger networks are more over-dimensioned (at least for the architectures evaluated here). We also observed that filters with the most channels are removed first, regardless of the architecture. This suggests that the high dimensional spaces of the three CNNs employed seem to be highly over-dimensioned for the task at hand. Furthermore, we found that using multiple input images to model identity of users strengthens the network, allowing higher pruning sparsities.

In future work, we are looking at other alternatives for network compression to further optimize the balance between network size and performance, such as pruning combined with Knowledge Distillation (KD). For example, the pruned networks could be trained to mimic the embedding of a more powerful one, e.g. [Deng et al., 2019a]. However, this would require that both the teacher and student networks have the same embedding size, which could be achieved by blocking pruning in the last convolutional layer. It has also been suggested that feature spaces of CNN trained in the same task can be linearly mapped [McNeely-White et al., 2020], which would solve the issue of embeddings of different size. The combination of several compression techniques, including quantization, KD and pruning, have also shown to be beneficial to achieve model reductions [Almadan and Rattani, 2023], and it will also be the source of future research.

Acknowledgments

This work was partly done while F. A.-F. was a visiting researcher at the University of the Balearic Islands. F. A.-F., K.

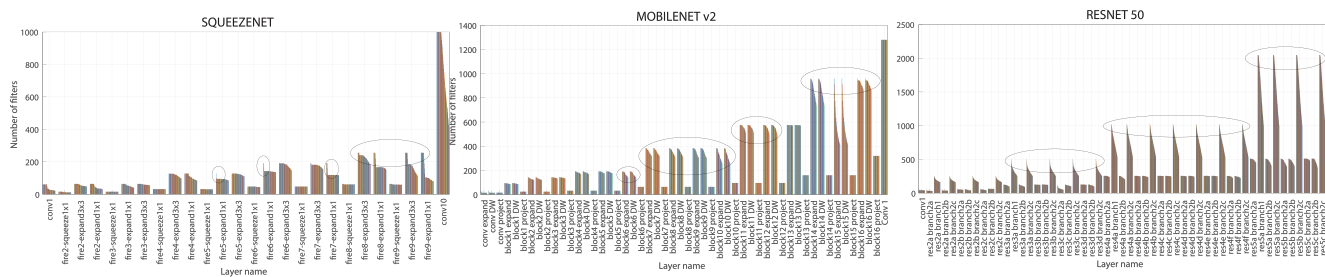


Fig. 8: Effect of pruning in the amount of filters per layer. For each layer, the y-axis indicate the amount of filters between 0% and 20% pruning. The circles indicate the layers with the fastest reduction in the amount of filters. The layer names correspond to the networks' release of Matlab r2023b.

H.-D., and J. B. thank the Swedish Research Council (VR) and the Swedish Innovation Agency (VINNOVA) for funding their research. Author J. M. B. thanks the project EXPLAINING - "Project EXPLAINable Artificial INtelligence systems for health and well-beING", under Spanish national projects funding (PID2019-104829RA-I00/AEI/10.13039/501100011033).

References

- A. Almadan and A. Rattani. Benchmarking neural network compression techniques for ocular-based user authentication on smartphones. *IEEE Access*, 11:36550–36565, 2023.
- F. Alonso-Fernandez, J. Barrachina, K. Hernandez Diaz, and J. Bigun. Squeeze-faceposenet: Lightweight face verification across different poses for mobile platforms. In *Proc. IAPR TC4 Workshop on Mobile and Wearable Biometrics, WMWB, in conjunction with ICPR*, 2020.
- Fernando Alonso-Fernandez, Kevin Hernandez-Diaz, Jose Maria Buades Rubio, and Josef Bigun. Squeezerfacenet: Reducing a small face recognition cnn even more via filter pruning. In *Proc. International Workshop on Artificial Intelligence and Pattern Recognition, IWAIPR*, pages 349–361, 2023.
- F. Boutros, N. Damer, M. Fang, F. Kirchbuchner, and A. Kuijper. Mixfacenets: Extremely efficient face recognition networks. In *2021 IEEE International Joint Conference on Biometrics, IJCB*, pages 1–8, 2021.
- F. Boutros, P. Siebke, M. Klemt, N. Damer, F. Kirchbuchner, and A. Kuijper. Pocketnet: Extreme lightweight face recognition network using neural architecture search and multistep knowledge distillation. *IEEE Access*, 10:46823–46833, 2022.
- Eduarda Caldeira, Pedro C. Neto, Marco Huber, Naser Damer, and Ana F. Sequeira. Model compression techniques in biometrics applications: A survey. *CoRR*, abs/2401.10139, 2024. URL <https://arxiv.org/abs/2401.10139>.
- Q. Cao, L. Shen, W. Xie, O. M. Parkhi, and A. Zisserman. Vggface2: A dataset for recognising faces across pose and age. In *13th IEEE International Conference on Automatic Face and Gesture Recognition, FG*, pages 67–74, 2018.
- S. Chen, Y. Liu, X. Gao, and Z. Han. Mobilefacenets: Efficient cnns for accurate real-time face verification on mobile devices. *CoRR*, abs/1804.07573, 2018. URL <http://arxiv.org/abs/1804.07573>.
- J. Deng, J. Guo, N. Xue, and S. Zafeiriou. Arcface: Additive angular margin loss for deep face recognition. In *IEEE/CVF Conference on Computer Vision and Pattern Recognition (CVPR)*, pages 4685–4694, 2019a.
- Jiankang Deng, Jia Guo, Yuxiang Zhou, Jinke Yu, Irene Kotsia, and Stefanos Zafeiriou. Retinaface: Single-stage dense face localisation in the wild. *CoRR*, abs/1905.00641, 2019b. URL <http://arxiv.org/abs/1905.00641>.
- C. N. Duong, K. G. Quach, I. K. Jalata, N. Le, and K. Luu. Mobiface: A lightweight deep learning face recognition on mobile devices. In *Proc IEEE 10th International Conference on Biometrics Theory, Applications and Systems, BTAS*, Sep. 2019.
- Yandong Guo, Lei Zhang, Yuxiao Hu, Xiaodong He, and Jianfeng Gao. Ms-celeb-1m: A dataset and benchmark for large-scale face recognition. In *14th European Conference on Computer Vision, ECCV*, pages 87–102, Cham, 2016. ISBN 978-3-319-46487-9.
- K. He, X. Zhang, S. Ren, and J. Sun. Deep residual learning for image recognition. In *Proc IEEE Conference on Computer Vision and Pattern Recognition, CVPR*, pages 770–778, June 2016.
- F. N. Iandola, M. W. Moskewicz, K. Ashraf, S. Han, W. J. Dally, and K. Keutzer. Squeezenet: Alexnet-level accuracy with 50x fewer parameters and <1mb model size. *CoRR*, abs/1602.07360, 2016. URL <http://arxiv.org/abs/1602.07360>.
- N. Jiang, Z. Xiong, H. Tian, X. Zhao, X. Du, C. Zhao, and J. Wang. Prune-facenet: Pruning lightweight face detection network by sparsity training. *Cognitive Computation and Systems*, 4(4):391–399, 2022.
- S. Kornblith, J. Shlens, and Q. V. Le. Do better imagenet models transfer better? In *Proc IEEE/CVF Conference on Computer Vision and Pattern Recognition (CVPR)*, pages 2656–2666, 2019.
- Jing Liu, Bohan Zhuang, Zhuangwei Zhuang, Yong Guo, Junzhou Huang, Jinhui Zhu, and Mingkui Tan. Discrimination-aware network pruning for deep model compression. *IEEE Transactions on Pattern Analysis and Machine Intelligence*, 44(8):4035–4051, 2022. doi: 10.1109/TPAMI.2021.3066410.
- Y. Martinez-Díaz, L. S. Luevano, H. Mendez-Vazquez, M. Nicolas-Diaz, L. Chang, and M. Gonzalez-Mendoza. Shufflefacenet: A lightweight face architecture for efficient and highly-accurate face recognition. In *Proc IEEE/CVF International Conference on Computer Vision Workshop, ICCVW*, pages 2721–2728, 2019.
- David G. McNeely-White, Benjamin Sattelberg, Nathaniel Blanchard, and J. Ross Beveridge. Common cnn-based face embedding spaces are (almost) equivalent. *CoRR*, abs/2010.02323, 2020. URL <https://arxiv.org/abs/2010.02323>.
- P. Molchanov, A. Mallya, S. Tyree, I. Frosio, and J. Kautz. Importance estimation for neural network pruning. In *IEEE/CVF Conference on Computer Vision and Pattern Recognition (CVPR)*, pages 11256–11264, 2019.
- Alice J. O'Toole, Carlos D. Castillo, Connor J. Parde, Matthew Q. Hill, and Rama Chellappa. Face space representations in deep convolutional neural networks. *Trends in Cognitive Sciences*, 22(9):794–809, 2018. ISSN 1364-6613. doi: 10.1016/j.tics.2018.06.006.
- Adam Polyak and Lior Wolf. Channel-level acceleration of deep face representations. *IEEE Access*, 3:2163–2175, 2015. doi: 10.1109/ACCESS.2015.2494536.
- Olga Russakovsky, Jia Deng, Hao Su, Jonathan Krause, Sanjeev Satheesh, Sean Ma, Zhiheng Huang, Andrej Karpathy, Aditya Khosla, Michael Bernstein, Alexander C. Berg, and Li Fei-Fei. Imagenet large scale visual recognition challenge. *International Journal of Computer Vision*, 115(3):211–252, Dec 2015. ISSN 1573-1405.
- M. Sandler, A. Howard, M. Zhu, A. Zhmoginov, and L. Chen. Mobilenetv2: Inverted residuals and linear bottlenecks. In *IEEE/CVF Conference on Computer Vision and Pattern Recognition, CVPR*, pages 4510–4520, 2018.
- K. Sundararajan and D. L. Woodard. Deep learning for biometrics: A survey. *ACM Comput. Surv.*, 51(3), May 2018. ISSN 0360-0300.
- M. Tan and Q. V. Le. Mixconv: Mixed depthwise convolutional kernels. In *30th British Machine Vision Conference, BMVC*, 2019.
- M. Yan, M. Zhao, Z. Xu, Q. Zhang, G. Wang, and Z. Su. Vargfacenet: An efficient variable group convolutional neural network for lightweight face recognition. In *IEEE/CVF International Conference on Computer Vision Workshops, ICCVW*, pages 2647–2654, 2019.
- Qian Zhang, Jianjun Li, Meng Yao, Liangchen Song, Helong Zhou, Zhichao Li, Wenming Meng, Xuezhi Zhang, and Guoli Wang. Vargnet: Variable group convolutional neural network for efficient embedded computing. *CoRR*, abs/1907.05653, 2020. URL <https://arxiv.org/abs/1907.05653>.
- X. Zhang, X. Zhou, M. Lin, and J. Sun. Shufflenet: An extremely efficient

convolutional neural network for mobile devices. In *Proc IEEE/CVF Conference on Computer Vision and Pattern Recognition, CVPR*, 2018.